Research Article

Investigation of rheological properties and conformation of cassava starch in zinc chloride solution[†]

Xiaodong Chen [1], Peng Liu [1,*] , Xiaoqin Shang [1], Fengwei Xie [2,**] , Huihua Jiang [1], Jie Wang [1],

[1]School of Chemistry and Chemical Engineering, Guangzhou University, Guangzhou 510006, China
[2]School of Chemical Engineering, The University of Queensland, Brisbane, Qld 4072, Australia

***Correspondence:** Dr. Peng Liu, School of Chemistry and Chemical Engineering, Guangzhou University, Guangzhou 510006, China; Email address: liu_peng@gzhu.edu.cn; Tel.: +86 15989006056; fax: +86 20 39366902.

****Correspondence:** Dr. Fengwei Xie, School of Chemical Engineering, The University of Queensland, Brisbane, Qld 4072, Australia. Email address: f.xie@uq.edu.au; fwhsieh@gmail.com, Tel.: +61 7 3346 3199.

[†]This article has been accepted for publication and undergone full peer review but has not been through the copyediting, typesetting, pagination and proofreading process, which may lead to differences between this version and the Version of Record. Please cite this article as doi:[10.1002/star.201600384].

Received: December 29, 2016 / Revised: February 13, 2017 / Accepted: April 12, 2017

ABSTRACT:

Zinc chloride aqueous solution is a non-derivatizing solvent for starch, and could be used as a media for homogeneous starch modification. This paper concerns the rheological properties of starch in $ZnCl_2$ aqueous solution under different conditions. Specifically, a large number (120) of viscosity-shear rate curves for starch-$ZnCl_2$ solutions with different starch contents, $ZnCl_2$ concentrations, and temperatures were obtained and modeled using a master curve method. In particular, the power-law index (*n*) from the modeling could accurately classify the starch molecules in $ZnCl_2$ aqueous solutions into an insoluble state, a dilute state, a semi-dilute state and a sticky state, reflecting the different degree of chain interactions in the solution. In particular, the sticky state would be mostly likely be controlled by the zinc-starch complex, which made the rheological behavior entirely different from that at low $ZnCl_2$ concentrations. The knowledge obtained from this study can be used to guide the homogeneous modification of starch and the fabrication of starch-based materials using green solvents such as aqueous $ZnCl_2$ with desired properties.

KEYWORDS: starch /zinc chloride /rheological modeling /phase diagram

Chemical compounds studied in this article:

Starch (PubChem CID: 24836924); Zinc Chloride (PubChem CID: 3007855); Water (PubChem CID: 962)

1Introduction

Starch is one of the most abundant biomacromolecules in nature[1, 2]. Due toits low cost, renewability, and biodegradability, starch has been widely used as a raw material in the industry[3, 4]. Furthermore, based on the abundant hydroxyl groups on its glucose units, native starch can be modified into various derivatives for the widened applications[5].For example, starch sodium succinate and starch phosphate ester can be used to prepare food additives; and starch can also be converted into value-added chemical products, such as binders and flocculants[6].

However, the modification of starch has been greatly limited by its insolubility in water and most organic solvents[7]. Starch, which is synthesized in the form of densely-packed heterogeneous granules[8, 9], shows low solubility in most conventional solvent despite being highly hydrophilic. As a result, starch is more resistant to various reactions than most of the other (in particular, synthetic) polymer, which can be easily dissolved in a solvent.

Recent research has been focused on the solvents for complete dissolution of starch. Regarding this, ionic liquids (ILs) represent a group of non-derivatizing solvents excellent for starch[10, 11]. Homogeneous systems based on ILs have been reported to be favorable for the chemical modification of starch into *e.g.* acetylated starch[12], cationic starch[13], and carboxymethyl starch[14] in 1-butyl-3-methylimidazoliumchloride ([Bmim]Cl);fatty-acid starch esters in 1-ethyl-3-methlyimidazolium acetate ([Emim][OAc])[15]; and for starch oxidation in a polyoxometalate (POM) IL[16]. All these studies have shown that ILs can be used to prepare modified starches with more desirable properties. However, the research on ILs has just been started and the toxicity of ILs remains uncertain. Moreover, the high prices of ILs restrict their practical application in industry. Therefore, the real potential of IL remains uncertain[5, 17].

Besides ILs, some salt solutions can also decrease the gelatinization temperature of starch, and accelerate the destruction of granules. Regarding this, these solutions have a "salt-in" effect[18], or the *Hofmeister* effect, which describes the fact that the presence of ions (especially anions) affects the solubility of macromolecules in aqueous solutions[19]. *Hofmeister* salts can generally be classified into two groups based on the different ions: the kosmotropes (the water structure makers or salt-out ions) and the chaotropes (the water structure breakers or salt-in ions). Jane *et al.*[20] further pointed out that because of the electro negative nature of starch, anions tend to repel starch -OH groups and stabilize starch granules; and cations, on the other hand, attract starch -OH groups and destabilize starch granules. Moreover, undercertain concentrations, LiCl, KSCN, KI, BaF_2, and $BaBr_2$ solutions can be used to gelatinize starch granules even at room temperature[21, 22]. In our previous study, $ZnCl_2$ aqueous solution was revealed to be a good non-derivatizing solvent for starch, and the dissolution mechanism was proposed to be the *Hofmeister* effect and the "zinc–starch complex"[5]. However, despite the scientific importance for practical applications, the conformation of starch macromolecules in salt solutions such as aqueous $ZnCl_2$ has seldom been reported so far.

In this work, we studied the rheological properties under different conditions to understand the conformation of starch chains in $ZnCl_2$aqueous solution. Cassava starch was chosen as it is commonly used as an industrial raw material. Based on the rheological results, we not only obtained a regressed power-law model to describe the rheological properties accurately, but also proposed a phase diagram describing the aggregation structure of starch molecules in $ZnCl_2$ solution.

2Materials and Methods

2.1 Materials

Native cassava starch was purchased from Dongguan Wenying Starch Trade Co., Ltd. (Guangzhou, China). Anhydrous zinc chloride ($ZnCl_2$, analytic grade) was supplied by Guangzhou Chemical Reagent Factory (Guangzhou, China). The distilled water was prepared in laboratory.

2.2 Preparation of starch-zinc chloride solutions

Certain amounts of anhydrous $ZnCl_2$ were added to a three-neck, round-bottom flask equipped with an electric stirrer to obtain $ZnCl_2$ aqueous solutions of certain concentrations (65%, 45%, 35% and 29.6wt.%). 29.6% was the critical concentration below which the starch could not be fully dissolved. 65% was the concentration that approaches to saturation. The other two concentrations, 35% and 45%, were used to enlarge the differences between samples. The $ZnCl_2$solution was then mixed with a certain amount of starch (1, 2, 3, 4, and 5wt.%, dry weight). Afterward, the system was stirred at 50°C for 4 h to achieve complete dissolution[5].

2.3 Rheological measurements of starch-$ZnCl_2$ solutions

The rheological measurements were carried out on a TA Discovery-DHR-2 rheometer (U.S.A.) with a 60 mm diameter plate-plate geometry and a Peltier temperature control system. For $ZnCl_2$ aqueous solutions of different concentrations, the steady shear experiments were carried out with the shear rate from 10 s^{-1} to 500 s^{-1} at various temperatures (25°C, 30°C, 40°C, 50°C, and 60°C). For starch-$ZnCl_2$ solutions, the same test parameters were used as for $ZnCl_2$ aqueous solutions, except that the shear rate was from 10 s^{-1} to 1000 s^{-1}. At this range of shear rate, the solutions were in a

pseudo-plastic state. Silicone oil (DC 200, Sigma-Aldrich) was placed around the edge of the measuring cell to prevent the absorption of moisture from the environment. Silicone oil would hardly affect the experimental results, as it is not miscible with polysaccharide solutions and has a relatively lower viscosity (9.5 mPa·s at 20°C).

All the rheological tests were carried out at least twice. For each sample at a certain condition, we compared the rheological curves from repeated tests. If the curves were very close to each other, a typical one was selected for use in the figures. If the curves had the significant differences, more repeats were undertaken.

2.4 Data analysis

The Microsoft®Excel software was used to carry out the linear regression based on a modified power-law equation and to obtain the correlation coefficients (R^2). Data were analyzed using a one way analysis of variance (ANOVA) and a Duncan's test for a statistical significance $P \leqslant 0.05$, using the SPSS Statistics 19.0.

3Results and discussion

3.1 Rheological proprieties of starch in $ZnCl_2$aqueous solution

In this work, we obtained 100 rheological (viscosity vs. shear rate) curves for starch-$ZnCl_2$solutions, and 20 curves for $ZnCl_2$ aqueous solutions (without starch), under different conditions. Some typical curves for starch-$ZnCl_2$ solutions were chosen to be illustrated in Fig. 1. Moreover, all parameters for 120 curves were illustrated in Table 1, Table 2, Table 3 and Table 4. In Fig.1, all the samples in the

shear rate range in question (10 s^{-1}–1000 s^{-1}) showed a shear-thinning behavior, and could be considered as pseudo-plastic fluids. This shear-thinning behavior of starch has also been reported in other solvents such as water, DMSO and NMMO [23-25].

From Fig. 1a, it could be seen that under the same $ZnCl_2$ concentration, the solution viscosity was increased with the increased starch content, and decreased with a higher temperature. From Fig. 1b and c, the viscosity was increased with the $ZnCl_2$ content and decreased with the increased temperature. Moreover, these results were as expected. All of the other rheological curves not shown here had the similar trends.

Moreover, for all the samples, a linear relationship between viscosity and shear rate can be seen on the double-logarithmic plot, indicating that a power-law model could be used to describe the rheological behaviors of starch-$ZnCl_2$ solutions [26-29]:

$$\eta = K \cdot \dot{\gamma}^{n-1} \qquad (1)$$

where η is the viscosity (Pa·s) of mixed solutions, $\dot{\gamma}$ is the shear rate (s^{-1}), K is the consistency (Pa·s), and n is the power-law index. For a pseudo-plastic solution, $n< 1$; the closer n was to1, the more Newtonian behavior the solution shows.

The detailed parameters of regression power-law equations for different $ZnCl_2$ aqueous solutions and starch-$ZnCl_2$ solutions can be seen from Table 1 to Table 4, respectively. It can be seen that nearly all correlation coefficients (R^2) were higher than 0.9, showing a strong power-law dependence of viscosity on shear rate.

The n values for the $ZnCl_2$ solutions at different conditions are illustrated in Fig. 2. For $ZnCl_2$ aqueous solutions (without starch), n was increased with the increased $ZnCl_2$ content and decreased with an increase in temperature. This suggests that the solution with more Zn^{2+} and Cl^- ions showed

a stronger Newtonian behavior (or the shear stability behavior); and the solution at a higher temperature would display a weaker Newtonian behavior (or the shear thinning behavior), which can be ascribed to the *Hofmeister* effect. This behavior was on the opposite with other conventional solutions and molten macromolecules. It is generally accepted that water is a Newtonian fluid, with *n* equals 1. But Cl^- is a strong chaotropes anion (or the structure breaker anions) to break the natural structure of water (which is described as the water cluster), and increase free water[20, 30]. Therefore, more Cl^- anions in the solution and/or a high temperature would contribute to a greater effect of Cl^- anions, *i.e.*, a stronger *Hofmeister* effect, resulting in more free water molecules. Thus, the solution had a weaker Newtonian behavior.

From Fig. 2, it could also be seen that irrespective of starch content, *n* was always decreased with the increased temperature when the $ZnCl_2$concentration was low (≤45%). This suggests that at low $ZnCl_2$ contents, the rheological properties of starch-$ZnCl_2$ solutions were mainly contributed by $ZnCl_2$ aqueous solutions, but not the concentration of starch macromolecules. This was reasonable considering the very low content of starch compared with Zn^{2+} and Cl^- contents in the solutions. However, when the $ZnCl_2$ concentration was high (65%) and the starch content was 2–5%, *n* was increased with a higher temperature, which was the same as conventional solutions and molten macromolecules. This indicates that, at these conditions, the rheological properties of the solution were influenced more by starch macromolecules but less by Zn^{2+} and Cl^- ions. These results could reflect the different degree of entanglement between starch molecules in solutions. Under the same starch content, the interaction and entanglement between starch macromolecules could be stronger at high $ZnCl_2$ contents than those at low $ZnCl_2$ contents. This result can be explained by the

"zinc-starch complex", which had been proposed by former researchers [5, 31]. The interaction between, and conformation of, starch molecules will be further discussed in Section 3.3.

3.2 Rheological model for starch in $ZnCl_2$ aqueous solution

To better understand the rheological properties of starch-$ZnCl_2$ aqueous solutions, the previous models in terms of power-law parameters have been used with modification. The power-law index n can be expressed as Eq.(2)[26, 27]:

$$n = n_0 + \alpha_1 \cdot T + \alpha_2 \cdot C_{ZnCl_2} + \alpha_3 \cdot C_{St} + \alpha_{12} \cdot T \cdot C_{ZnCl_2} + \alpha_{13} \cdot T \cdot C_{St} + \alpha_{23} \cdot C_{ZnCl_2} \cdot C_{St} + \alpha_{123} \cdot T \cdot C_{ZnCl_2} \cdot C_{St} \quad (2)$$

where T is the absolute temperature (Kelvin) of the solution, C_{ZnCl_2} is the $ZnCl_2$ content (w/w, dry basis), C_{St} is the starch content (w/w, dry basis), and n_0, α_1, α_2, α_3, α_{12}, α_{13}, α_{23} and α_{123} are constants. By linear regression based on the 100 curves for starch-$ZnCl_2$ solutions, the constants are calculated: n_0 = 1.596, α_1=−0.00381, α_2= −0.984, α_3= 0.0816, α_{12}= 0.00541, α_{13}= 0.0000668, α_{23}= −0.351 and α_{123} = 0.000468. The correlation coefficient is 0.903, which is satisfactory.

The consistency K can be expressed using Eq.(3) [26, 28]:

$$K = K_0 \exp\left[\frac{E}{R}\left(\frac{1}{T}\right) - \alpha C_{ZnCl_2} - \alpha' C_{St}\right] \quad (3)$$

where E/R is the reduced flow activation energy (Kelvin) and K_0 is another constant (Pa·s^n). By linear regression on the 100 curves for starch-$ZnCl_2$ solutions, the constants are calculated: K_0 = 0.000213, E/R =1460, α=−2.544, and α'=−0.642. The correlation coefficient is 0.917, which is also satisfactory.

From these calculated constants, it is clear that the $ZnCl_2$ content had the greatest influence on both *n* and *K*. The impact of the starch content on these two parameters was small, and the impact of temperature on *n* was extremely weak.

The established rheological model for starch-$ZnCl_2$ solutions (starch content: 1%–5%; $ZnCl_2$ concentration: 29.6%–65%; temperature: 25°C–60°C) is expected to be useful to predict the rheological properties in other conditions.

3.3 Master curve study

For molten macromolecules, the master curve can be drawn using the classical time–temperature superposition, and it can also be extended to include other experimental parameters such as the plasticizer content[26, 27, 32]. Here, for starch-$ZnCl_2$ solutions, a master curve study can also involve the effects of starch content and $ZnCl_2$ content, which makes it possible to gather all the experimental data in this work for comparison purpose. The reduced viscosity, $\eta / \alpha_{T\cdot ZnCl_2\cdot St}$, can be plotted against the reduced shear rate, $\dot{\gamma}\cdot\alpha_{T\cdot ZnCl_2\cdot St}$,where $\alpha_{T\cdot ZnCl_2\cdot St}$ is the shift factor defined as Eq.(4).

$$\alpha_{T\cdot ZnCl_2\cdot St} = \exp\left[\frac{E}{R}\left(\frac{1}{T_i}-\frac{1}{T_0}\right)-\alpha\left(C_{ZnCl_2 i}-C_{ZnCl_2 0}\right)-\alpha'\left(C_{St i}-C_{St 0}\right)\right] \quad (4)$$

where the subscript *i* indicates the flow conditions to be superposed on the reference flow conditions, which is labeled by the subscript 0. Here, the reference conditions are: T_0 = 25°C, $C_{ZnCl_2 0}$ = 29.6%, and C_{St0} = 1%. The reduced curves can only be superposed if the molecules in different samples share the same structure and/or conformation.

Fig. 3a shows the master curves of starch-$ZnCl_2$ solutions with the same starch content (1%). It can be seen that in this case starch-$ZnCl_2$ solutions could be divided into two groups (labeled as G1

and G2). Group G1 represents samples with low $ZnCl_2$ concentrations (29.6%–45%), irrespective of the temperature (25–60°C). This shows that when the $ZnCl_2$ concentration was low, the conformation of starch molecules in solutions was similar. However, when the $ZnCl_2$ concentration reached 65% (G2), their reduced curves were separated from G1. These results can be seen in other starch contents (1–5%), which are not shown here. In agreement with the *n* results as discussed in Section 3.1, here, the results show that when the starch content was the same, the interaction and entanglement between starch macromolecules should be stronger at a high $ZnCl_2$ content (65%) than those at low $ZnCl_2$ contents (29.6%–45%). Again, this could be ascribed to the formation of a "zinc-starch complex". Specifically, Zn^{2+} can attract starch –OH groups[20]. As a result, Zn^{2+} played the role as a crosslinking agent and enhanced the interaction and entanglement between starch chains. Moreover, the high content of Zn^{2+} resulted in the much more formation of zinc-starch complex, and the more entanglement. Therefore, at a high concentration of Zn^{2+} ions, the starch molecules influenced the rheological properties more strongly, and their conformation was different from that with low Zn^{2+} contents, which causes the separation of master curves.

Fig. 3b shows the reduced curves under the same $ZnCl_2$ contents (29.6% and 35%). It can be observed that in these cases starch-$ZnCl_2$ solutions can also be divided into two groups, with the starch content being 1% (G1), and 2% to 5% (G2), respectively. In other words, the reduced curves for 1% starch content stayed apart from others. This phenomenon can also be seen for the curves for 45% $ZnCl_2$ content, which are not shown here. We propose the reason causing the master curve separation was the different degree of entanglement of starch chains and starch-zinc complex. Specifically, at 1% starch content, there was limited entanglement between starch chains and starch-zinc complex, which were dispersed individually. However, a high starch content could lead to

greater entanglement between starch chains and starch-zinc complex. A similar phenomenon have been observed in a previous study[25] for waxy starch in an ionic liquid 1-ethyl-3-methylimidazolium acetate ([Emim][OAc]), where the conformation of starch molecules as reflected by rheological results could be classified into either a "dilute region" or a "semi-dilute region". In their study, the critical starch concentration between the dilute region and the semi-dilute region was also 1%.

3.4 Phase diagram and schematic representation of the conformation of starch macromolecules in $ZnCl_2$ aqueous solution

Based on the above discussion in Sections 3.1 and 3.3, Fig. 4 shows a phase diagram with schematic representation of the conformation of starch macromolecules. In Fig. 4, there are four regions in the phase diagram: Phase I represents an "insoluble region"; Phase II represents a "dilute region"; Phase III represents a "semi-dilute region"; and Phase IV accounts for a "sticky region". Specifically, when the content of $ZnCl_2$ was lower than 29.6% (the red part), starch could not dissolve in the solution and exists as granules (Phase I, the insoluble region)[5]. When the $ZnCl_2$ concentration was between 29.6% to 65%, and the starch content was lower than 1% (the purple part), the starch chains were dispersed individually in the solution, without entanglement (Phase II, the dilute region). When the $ZnCl_2$ concentration was still 29.6%–65%, but the content of starch was between 2% to 5% (the green part), there were apparent interaction and entanglement between starch molecules, which had the same conformation (Phase III, the semi-dilute region). Moreover, when the $ZnCl_2$ concentration was ≥65% and the content of starch was more than 1% (the blue part), the "zinc-starch complex" was formed and had the much stronger interaction and entanglement than those between pure starch

chains (Phase IV, the sticky region). This complex could much more strongly influence the rheological properties of solutions than the $ZnCl_2$ aqueous solution itself. Besides, when the $ZnCl_2$ concentration was 29.6%–65%, but the content of starch was between ≥5%, from the rheological information, it should also be classified to the "sticky region" (Phase IV, the blue part), because of the high entanglement between starch chains.

This phase diagram summarizes the existence of starch molecules in $ZnCl_2$ solutions, and can be used to guide the homogeneous modification of starch. For example, in the dilute region, the starch chains disperse widely and the entanglement is weak, it is suitable for those modified reactions with a high degree of substitution.

3.5 Modified master curves for confirmation of the phase diagram

Based on the proposed phase diagram (Fig. 4), the 100 rheological curves for starch-$ZnCl_2$ solutions under different conditions were classified into three groups respectively: 60 curves belong to the semi-dilute region ($ZnCl_2$ content: 29.6%–45%; starch content: 2%–5%; and temperature: 25–60°C); 15 curves belong to the dilute region ($ZnCl_2$ content: 29.6%–45%; starch content: 1%; temperature: 25–60°C); and 25 curves belong to the sticky region ($ZnCl_2$ content: 65%; starch content: 2%–5%; temperature: 25–60°C). For each group, the shift factor ($\alpha_{T\cdot ZnCl2\cdot St}$) was re-calculated using Eq. 4. As a result, the re-built master curves for each group were seen in Fig. 5.

Fig. 5a shows the 15 re-built reduced curves in the dilute region. Here, the reference conditions are: T_0 = 25°C, C_{ZnCl20} = 29.6%, and C_{St0} = 1%. All these curves were superposed, without separation. Initially, we included five more curves ($ZnCl_2$content: 65%; starch content: 1%; temperature: 25°C,

30°C, 40°C, 50°C, 60°C) into this region. However, after re-establishment, these five reduced curves were found to be better classified into the sticky region.

Fig. 5b contains the typical 24 re-built reduced curves in the semi-dilute region, which represent all of the 60 curves. Here, the reference conditions are: T_0 = 25 °C, C_{ZnCl20} = 29.6%, andC_{St0} = 2%. Although the dispersity of these curves is much more than that in Fig. 5a and Fig. 5c, there was still no obvious separation. Moreover, the dispersity just indicates a gradual and moderate change of the conformation of starch molecules in $ZnCl_2$ solution.

Fig. 5c shows the 25 re-built reduced curves in the sticky region. Here, the reference conditions are: T_0 = 25 °C, C_{ZnCl20} = 65%, andC_{St0} = 1%. Similarly as in Fig. 5a, all the curves were superposed, without separation.

From the re-built master curves in Fig. 5, the proposed phase diagram is confirmed.

4Conclusions

We previously found that $ZnCl_2$ aqueous solution was a non-derivatizing solvent that can completely dissolve starch. Here in this work, we further studied the rheological and conformation of starch molecules in $ZnCl_2$ aqueous solution under different conditions. In fact, besides rheological studies, we have tried the gel permeation chromatography (GPC) to study the conformation. However, because of the high salt concentration, which may damage the chromatographic column of GPC, is the key parameter for the dissolution and dispersion of starch chains. We got nothing from it.

For the purpose, we obtained 100 rheological curves for starch-$ZnCl_2$ solutions and established a rheological model to describe the rheological properties under different conditions accurately. More importantly, our power-law index (n) and master curve studies allow us to classify the

conformation of starch molecules in $ZnCl_2$aqueous solutions into a dilute region, a semi-dilute region, a sticky region, and an insoluble region, which can be shown in a phase diagram. In the dilute region, the starch chains are dispersed individually in the solution, without entanglement. In the semi-dilute region, there were strong interaction and entanglement between starch molecules. In the sticky region, the zinc-starch complex was formed and had the much stronger interaction and entanglement than those between pure starch chains. This phase diagram can be used to guide the homogeneous modification of starch and the preparation of starch-based materials with desired structure and properties.

The research leading to these results has received fundingfrom the National Natural Science Foundation of China (NSFC)(Project Nos. 21106023 and 31271942), the "Science and Technology Planning Project of Guangdong Province" (2016A010103044 and 2013B010403030), the "Science and Technology Projects supportedby Guangzhou Education Bureau" (Project No. 1201410965), andthe "Pearl River S&T Nova Program of Guangzhou" (Project No.201610010019). Besides, the authors also thank for the financial support provided by "The Foundation for Fostering the Scientific and Technical Innovation of Guangzhou University".

The authors have declared no conflict of interest.

References

[1] Yang, J., Xie, F., Wen, W., Chen, L.*, et al.*, Understanding the structural features of high-amylose maize starch through hydrothermal treatment. *International journal of biological macromolecules* 2016, *84*, 268-274.

[2] Tang, Y., Xie, F., Zhang, D., Zhu, M.*, et al.*, Physical properties and prebiotic activity of maize starch-based functional films. *Starch - Stärke* 2015, *67*, 124-131.

[3] Neelam, K., Vijay, S., Lalit, S., Various techniques for the modification of starch and the applications of its derivatives. *International Research Journal of Pharmacy* 2012, *3*, 25-31.

[4] Xie, F., Pollet, E., Halley, P. J., Avérous, L., Starch-based nano-biocomposites. *Progress in Polymer Science* 2013, *38*, 1590-1628.

[5] Lin, M., Shang, X., Liu, P., Xie, F.*, et al.*, Zinc chloride aqueous solution as a solvent for starch. *Carbohydrate Polymers* 2016, *136*, 266-273.

[6] Wu, D., Hakkarainen, M., A closed-loop process from microwave-assisted hydrothermal degradation of starch to utilization of the obtained degradation products as starch plasticizers. *ACS Sustainable Chemistry & Engineering* 2014, *2*, 2172-2181.

[7] Junistia, L., Sugih, A. K., Manurung, R., Picchioni, F.*, et al.*, Synthesis of higher fatty acid starch esters using vinyl laurate and stearate as reactants. *Starch ‐ Stärke* 2008, *60*, 667-675.

[8] Buléon, A., Colonna, P., Planchot, V., Ball, S., Starch granules: structure and biosynthesis. *International journal of biological macromolecules* 1998, *23*, 85-112.

[9] Sciarini, L., Rolland-Sabaté, A., Guilois, S., Decaen, P.*, et al.*, Understanding the destructuration of starch in water–ionic liquid mixtures. *Green Chemistry* 2015, *17*, 291-299.

[10] Jordan, T., Schmidt, S., Liebert, T., Heinze, T., Molten imidazole – a starch solvent. *Green Chemistry* 2014, *16*, 1967-1973.

[11] Papanyan, Z., Roth, C., Wittler, K., Reimann, S., Ludwig, R., The dissolution of polyols in salt solutions and ionic liquids at molecular level: ions, counter ions, and Hofmeister effects. *ChemPhysChem* 2013, *14*, 3667-3671.

[12] Biswas, A., Shogren, R. L., Stevenson, D. G., Willett, J. L., Bhowmik, P. K., Ionic liquids as solvents for biopolymers: Acylation of starch and zein protein. *Carbohydrate Polymers* 2006, *66*, 546-550.

[13] Wang, Y., Xie, W., Synthesis of cationic starch with a high degree of substitution in an ionic liquid. *Carbohydrate Polymers* 2010, *80*, 1172-1177.

[14] Xie, W., Zhang, Y., Liu, Y., Homogenous carboxymethylation of starch using 1-butyl-3-methylimidazolium chloride ionic liquid medium as a solvent. *Carbohydrate Polymers* 2011, *85*, 792-797.

[15] Gao, J., Luo, Z. G., Luo, F. X., Ionic liquids as solvents for dissolution of corn starch and homogeneous synthesis of fatty-acid starch esters without catalysts. *Carbohydrate Polymers* 2012, *89*, 1215-1221.

[16] Chen, X., Souvanhthong, B., Wang, H., Zheng, H.*, et al.*, Polyoxometalate-based Ionic liquid as thermoregulated and environmentally friendly catalyst for starch oxidation. *Applied Catalysis B: Environmental* 2013, *138-139*, 161-166.

[17] Mateyawa, S., Xie, D. F., Truss, R. W., Halley, P. J.*, et al.*, Effect of the ionic liquid 1-ethyl-3-methylimidazolium acetate on the phase transition of starch: Dissolution or gelatinization? *Carbohydrate polymers* 2013, *94*, 520-530.

[18] Bogar, F., Bartha, F., Nasztor, Z., Fabian, L.*, et al.*, On the Hofmeister effect: fluctuations at the protein-water interface and the surface tension. *The journal of physical chemistry. B* 2014, *118*, 8496-8504.

[19] Hofmeister, F., Naunyn-Schmiedeberg's Arch. *Exp. Pathol. Pharmakol.(Leipzig)* 1888, *24*, 247.

[20] Jane, J. L., Mechanism of starch gelatinization in neutral salt solutions. *Starch ‐ Stärke* 1993, *45*, 161-166.

[21] Ahmad, F. B., Williams, P. A., Effect of salts on the gelatinization and rheological properties of sago starch. *Journal of agricultural and food chemistry* 1999, *47*, 3359-3366.

[22] Lai, V. M. F., Tomasik, P., Yen, M. T., Hung, W. L., Lii, C. y., Re ‐ examination of the interactions between starch and

salts of metals from the non‐transition groups. *International journal of food science & technology* 2001, *36*, 321-330.
[23] De Vasconcelos, C., Pereira, M., Fonseca, J., Solvent composition and rheology of starch–DMSO–water solutions. *J Appl Polym Sci* 2001, *80*, 1285-1290.
[24] Koganti, N., Mitchell, J. R., Ibbett, R. N., Foster, T. J., Solvent effects on starch dissolution and gelatinization. *Biomacromolecules* 2011, *12*, 2888-2893.
[25] Liu, W., Budtova, T., Dissolution of unmodified waxy starch in ionic liquid and solution rheological properties. *Carbohydrate polymers* 2013, *93*, 199-206.
[26] Tajuddin, S., Xie, F., Nicholson, T. M., Liu, P., Halley, P. J., Rheological properties of thermoplastic starch studied by multipass rheometer. *Carbohydrate Polymers* 2011, *83*, 914-919.
[27] Della Valle, G., Colonna, P., Patria, A., Vergnes, B., Influence of amylose content on the viscous behavior of low hydrated molten starches. *Journal of Rheology* 1996, *40*, 347-362.
[28] Martin, O., Averous, L., Della Valle, G., In-line determination of plasticized wheat starch viscoelastic behavior: impact of processing. *Carbohydrate Polymers* 2003, *53*, 169-182.
[29] Xie, W., Shao, L., Phosphorylation of Corn Starch in an Ionic Liquid. *Starch - StÃ¤rke* 2009, *61*, 702-708.
[30] Evans, I., Haisman, D., The effect of solutes on the gelatinization temperature range of potato starch. *Starch ‐ Stärke* 1982, *34*, 224-231.
[31] Cao, N. J., Xu, Q., Chen, C. S., Gong, C. S., Chen, L. F., Cellulose hydrolysis using zinc chloride as a solvent and catalyst. *Applied Biochemistry andBiotechnology, 45, 521–530.* 1994, *45*, 521-530.
[32] Vergnes, B., Della Valle, G., Tayeb, J., A specific slit die rheometer for extruded starchy products. Design, validation and application to maize starch. *Rheologica Acta* 1993, *32*, 465-476.

Figure Lgends

Fig. 1. Viscosity vs. shear rate curves of cassava starch in $ZnCl_2$ solutions. The particular parameter for curves was: (a) 29.6% $ZnCl_2$ concentration; (b) 1% starch content; (c) 25 °C.

Fig. 2. *n* values of regressed power-law equations for cassava starch in $ZnCl_2$ aqueous solution under different conditions ($ZnCl_2$ concentration, starch content, and temperature).

Fig. 3. Master curves of rheological results for cassava starch in $ZnCl_2$ aqueous solutions obtained by temperature–cassava starch content–$ZnCl_2$ content superposition. The regression conditions of were T_0=25 °C, C_{ZnCl20}=29.6%, and C_{St0}=1%. The particular parameter for curves was: (a) 1% starch content; (b) $ZnCl_2$ concentration (29.6% and 35%).

Fig. 4. Phase diagram and schematic representation for cassava starch in $ZnCl_2$ aqueous

solutions under different conditions. Phase I represents the “insoluble region”; Phase II represents the “dilute region”; Phase III represents the “semi-dilute region”; and Phase IV represents the “sticky region”.

Fig. 5. Re-built master curves for cassava starch in $ZnCl_2$ solvents in three phase regions. (a) dilute region; (b) semi-dilute region; and (c) sticky region.

Table 1. Power-law parameters for cassava starch in 29.6% $ZnCl_2$ aqueous solution.

Starch content	Temperature	n	K (Pa·s)	R^2
0%	25 °C	0.172[a]	0.878[c]	0.988
	30 °C	0.185[a]	0.829[d]	0.986
	40 °C	0.165[b]	0.898[b]	0.986
	50 °C	0.157[b]	0.922[b]	0.987
	60 °C	0.149[c]	0.935[a]	0.991
1%	25°C	0.689[a]	0.111[a]	0.963
	30 °C	0.672[b]	0.109[a]	0.961
	40 °C	0.660[c]	0.098[ab]	0.961
	50 °C	0.641[d]	0.096[c]	0.959
	60 °C	0.613[e]	0.101[ab]	0.965
2%	25 °C	0.755[a]	0.253[a]	0.945
	30 °C	0.744[b]	0.243[a]	0.949
	40 °C	0.729[c]	0.217[b]	0.959
	50 °C	0.712[d]	0.205[c]	0.966
	60 °C	0.681[e]	0.224[a]	0.986
3%	25 °C	0.762[a]	0.409[a]	0.917
	30 °C	0.754[b]	0.389[b]	0.936
	40 °C	0.735[b]	0.353[c]	0.957
	50 °C	0.722[c]	0.329[d]	0.971
	60 °C	0.699[d]	0.337[c]	0.989
4%	25 °C	0.753[a]	1.154[a]	0.982
	30 °C	0.761[a]	1.009[b]	0.979
	40 °C	0.763[a]	0.805[c]	0.973
	50 °C	0.762[a]	0.696[d]	0.967
	60 °C	0.757[a]	0.597[e]	0.968
5%	25 °C	0.832[a]	0.983[a]	0.881
	30 °C	0.835[a]	0.872[b]	0.872

40 °C	0.820[b]	0.770[c]	0.939
50 °C	0.826[b]	0.623[d]	0.855
60 °C	0.804[c]	0.635[d]	0.896

Superscripts with different letters in same column indicate significant differences ($P \leqslant 0.05$).

Table 2. Power-law parameters for cassava starch in 35% $ZnCl_2$ aqueous solution.

Starch content	Temperature	n	K (Pa·s)	R^2
0%	25 °C	0.192^{a}	0.811^{d}	0.987
	30 °C	0.197^{a}	0.793^{e}	0.985
	40 °C	0.182^{b}	0.833^{c}	0.987
	50 °C	0.164^{b}	0.889^{b}	0.988
	60 °C	0.151^{c}	0.940^{a}	0.988
1%	25 °C	0.693^{a}	0.121^{a}	0.969
	30 °C	0.687^{a}	0.114^{b}	0.966
	40 °C	0.676^{a}	0.102^{c}	0.961
	50 °C	0.693^{a}	0.080^{d}	0.974
	60 °C	0.641^{a}	0.099^{cd}	0.962
2%	25 °C	0.734^{a}	0.264^{a}	0.983
	30 °C	0.727^{a}	0.243^{b}	0.985
	40 °C	0.715^{a}	0.215^{c}	0.989
	50 °C	0.702^{a}	0.200^{d}	0.990
	60 °C	0.676^{a}	0.211^{c}	0.996
3%	25 °C	0.765^{a}	0.436^{a}	0.934
	30 °C	0.759^{a}	0.404^{b}	0.947
	40 °C	0.737^{b}	0.378^{c}	0.967
	50 °C	0.735^{b}	0.332^{e}	0.982
	60 °C	0.704^{c}	0.362^{d}	0.994
4%	25 °C	0.808^{a}	0.667^{a}	0.900
	30 °C	0.802^{b}	0.612^{b}	0.899
	40 °C	0.744^{d}	0.559^{c}	0.920
	50 °C	0.777^{c}	0.497^{d}	0.937
	60 °C	0.735^{d}	0.561^{c}	0.971
5%	25 °C	0.823^{a}	0.979^{a}	0.896
	30 °C	0.821^{ab}	0.884^{b}	0.891

40 °C	0.813^{bc}	0.751^{c}	0.888
50 °C	0.798^{c}	0.698^{d}	0.924
60 °C	0.765^{d}	0.762^{c}	0.945

Superscripts with different letters in same column indicate significant differences ($P \leqslant 0.05$).

Table 3. Power-law parameters for cassava starch in 45% $ZnCl_2$ aqueous solution.

Starch content	Temperature	n	K (Pa·s)	R^2
0%	25 °C	0.229[a]	0.730[d]	0.982
	30 °C	0.211[b]	0.775[c]	0.984
	40 °C	0.198[b]	0.81[1b]	0.981
	50°C	0.189[c]	0.814[b]	0.987
	60°C	0.166[d]	0.895[a]	0.986
1%	25 °C	0.714[a]	0.142[a]	0.981
	30 °C	0.717[a]	0.126[b]	0.982
	40 °C	0.703[ab]	0.113[bc]	0.976
	50 °C	0.691[bc]	0.106[cd]	0.969
	60 °C	0.677[d]	0.101[d]	0.972
2%	25 °C	0.752[a]	0.353[a]	0.974
	30 °C	0.747[b]	0.329[b]	0.978
	40 °C	0.737[bc]	0.284[c]	0.982
	50 °C	0.722[cd]	0.264[d]	0.987
	60 °C	0.712[d]	0.248[d]	0.990
3%	25 °C	0.780[a]	0.755[a]	0.959
	30 °C	0.779[ab]	0.681[b]	0.957
	40 °C	0.774[ab]	0.573[c]	0.948
	50 °C	0.769[bc]	0.502[d]	0.955
	60 °C	0.758[c]	0.471[e]	0.975
4%	25 °C	0.781[a]	1.414[a]	0.971
	30 °C	0.789[a]	1.237[b]	0.967
	40 °C	0.788[a]	1.002[c]	0.960
	50 °C	0.786[a]	0.859[d]	0.953
	60 °C	0.774[b]	0.822[e]	0.969
5%	25 °C	0.763[b]	2.256[a]	0.981
	30 °C	0.769[ab]	1.948[b]	0.982

	40 °C	0.778[a]	1.502[c]	0.981
	50 °C	0.775[a]	1.288[d]	0.979
	60 °C	0.769[ab]	1.200[e]	0.983

Superscripts with different letters in same column indicate significant differences ($P \leqslant 0.05$).

Table 4. Power-law parameters for cassava starch in 65% $ZnCl_2$ aqueous solution.

Starch content	Temperature	*n*	*K* (Pa·s)	R^2
0%	25 °C	0.571^{a}	0.429^{e}	0.953
	30 °C	0.523^{b}	0.477^{d}	0.965
	40 °C	0.491^{c}	0.509^{c}	0.969
	50 °C	0.435^{d}	0.565^{b}	0.975
	60 °C	0.408^{e}	0.592^{a}	0.977
1%	25 °C	0.842^{a}	0.177^{a}	0.994
	30 °C	0.841^{a}	0.154^{b}	0.989
	40 °C	0.839^{ab}	0.119^{c}	0.973
	50 °C	0.836^{ab}	0.096^{d}	0.957
	60 °C	0.826^{b}	0.083^{e}	0.932
2%	25 °C	0.797^{b}	0.569^{a}	0.996
	30 °C	0.807^{a}	0.472^{b}	0.990
	40 °C	0.816^{a}	0.345^{c}	0.992
	50 °C	0.827^{a}	0.260^{d}	0.993
	60 °C	0.829^{a}	0.209^{e}	0.995
3%	25 °C	0.753^{d}	1.622^{a}	0.990
	30 °C	0.761^{d}	1.344^{b}	0.988
	40 °C	0.776^{c}	0.948^{c}	0.988
	50 °C	0.786^{ab}	0.708^{d}	0.992
	60 °C	0.798^{a}	0.543^{e}	0.991
4%	25 °C	0.719^{c}	3.322^{a}	0.990
	30 °C	0.721^{c}	3.133^{b}	0.994
	40 °C	0.744^{b}	1.986^{c}	0.983
	50 °C	0.758^{a}	1.460^{d}	0.981
	60 °C	0.768^{a}	1.134^{e}	0.983
5%	25 °C	0.691^{bc}	6.637^{a}	0.992
	30 °C	0.689^{c}	5.743^{b}	0.997

40 °C	0.696[b]	4.347[c]	0.996
50 °C	0.726[a]	2.912[d]	0.985
60 °C	0.725[a]	2.362[e]	0.992

Superscripts with different letters in same column indicate significant differences ($P \leqslant 0.05$).

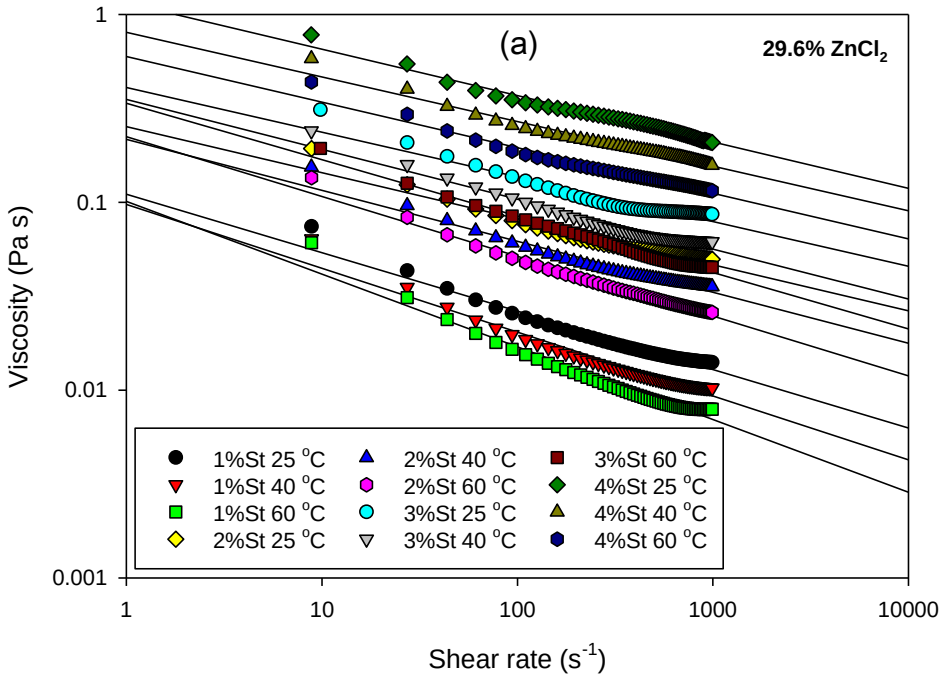

s

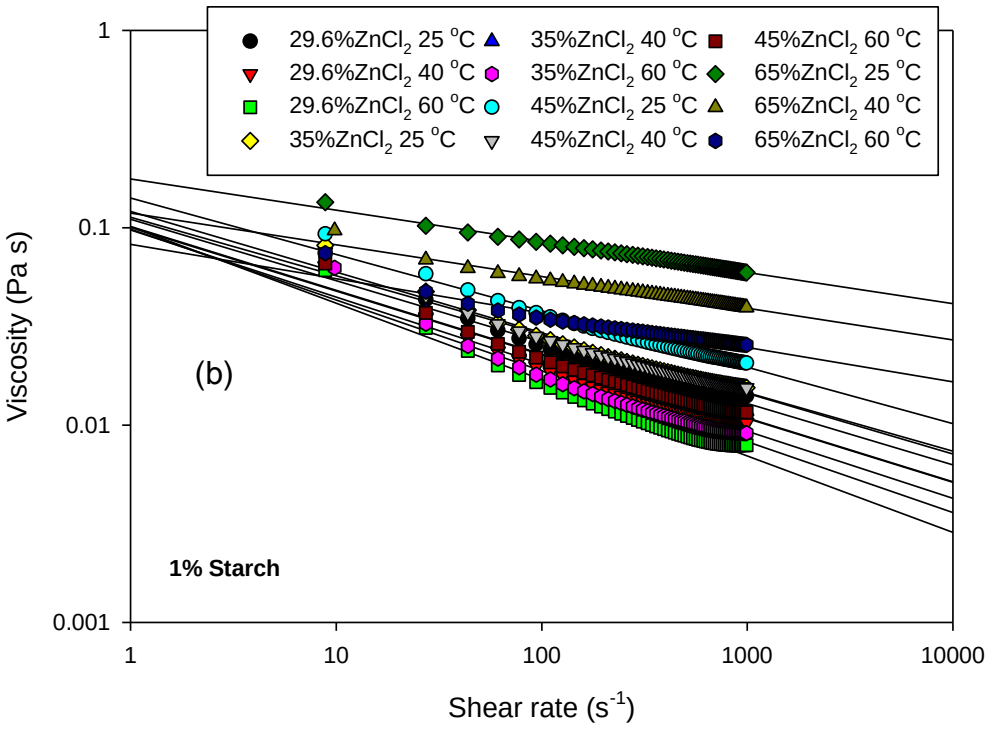

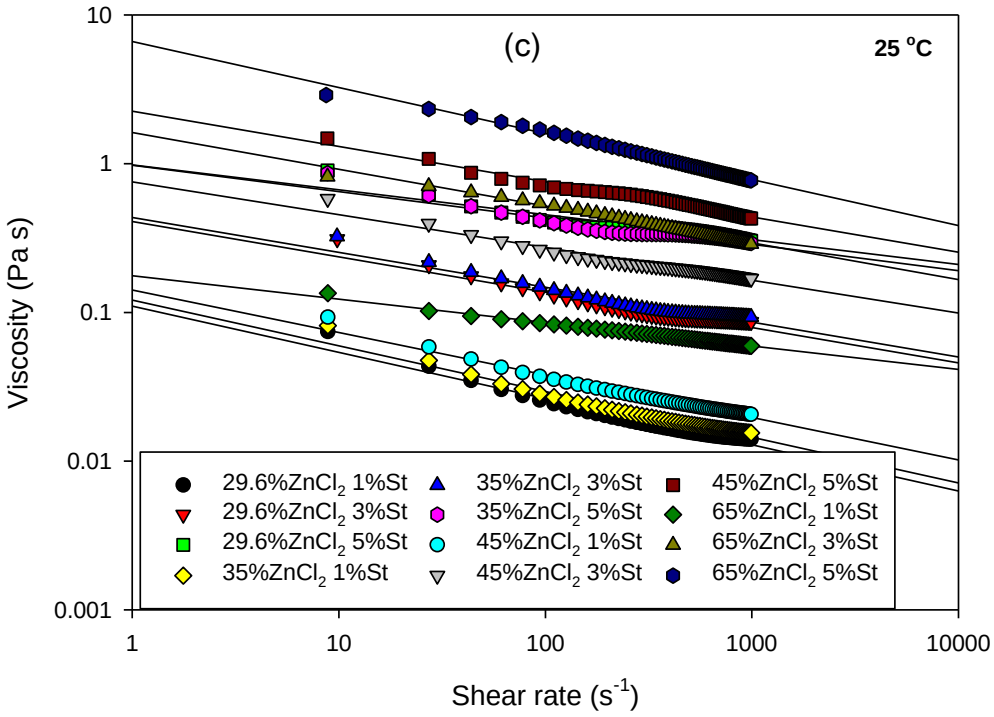

Fig. 1. Viscosity vs. shear rate curves of cassava starch in $ZnCl_2$ solutions. The particular parameter for curves was: (a) 29.6% $ZnCl_2$ concentration; (b) 1% starch content; (c) 25 °C.

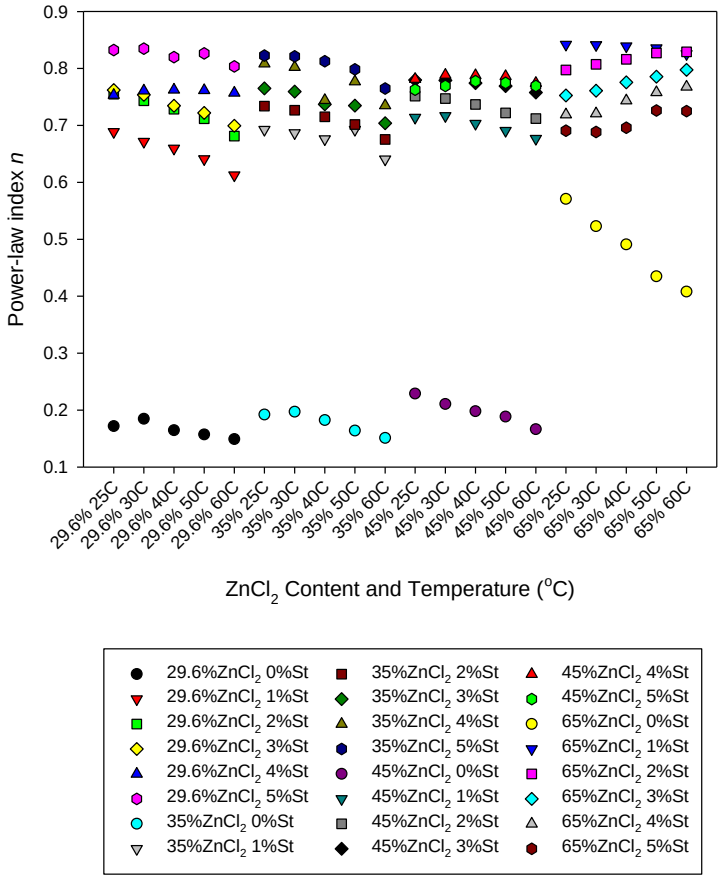

Fig. 2. *n* values of regressed power-law equations for cassava starch in $ZnCl_2$ aqueous solution under different conditions ($ZnCl_2$ concentration, starch content, and temperature).

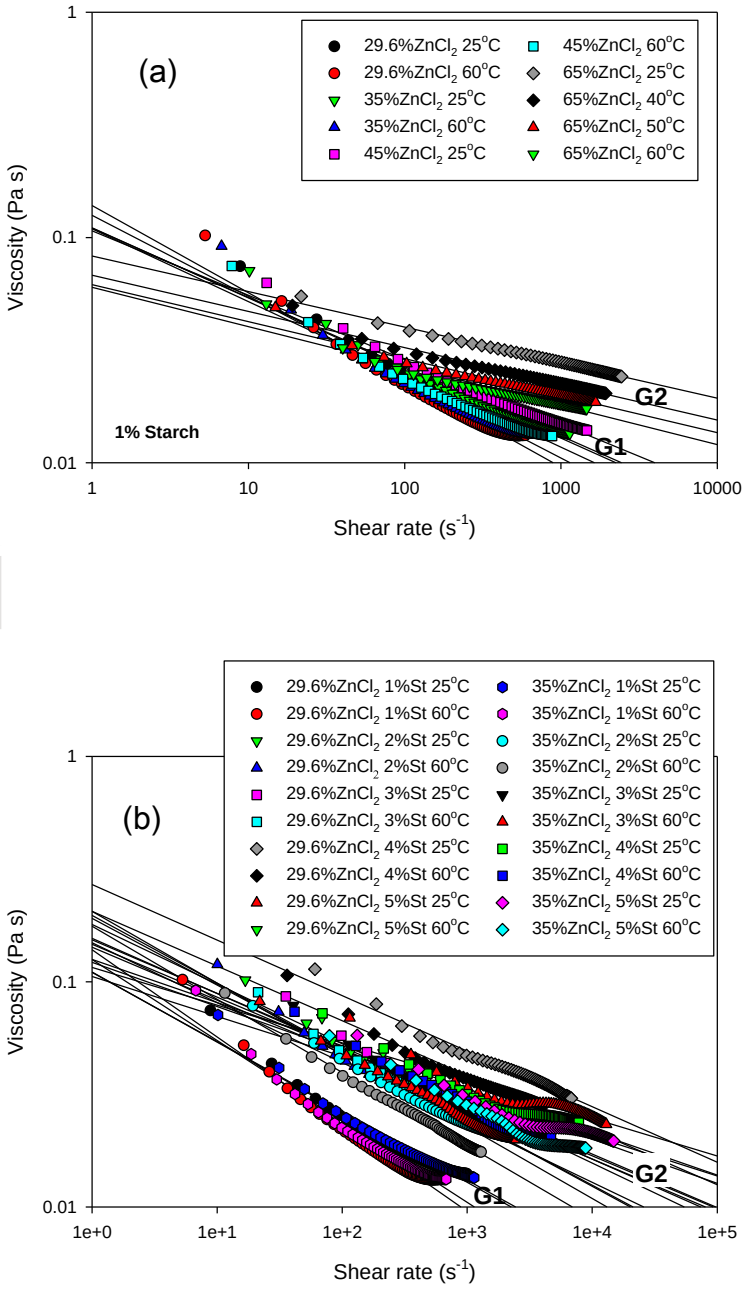

Fig. 3. Master curves of rheological results for cassava starch in $ZnCl_2$aqueous solutions obtained by temperature–cassava starch content–$ZnCl_2$ content superposition. The regression conditions of were T_0=25 °C, C_{ZnCl20}=29.6%, and C_{St0}=1%. The particular parameter for curves was: (a) 1% starch content; (b) $ZnCl_2$ concentration (29.6% and 35%).

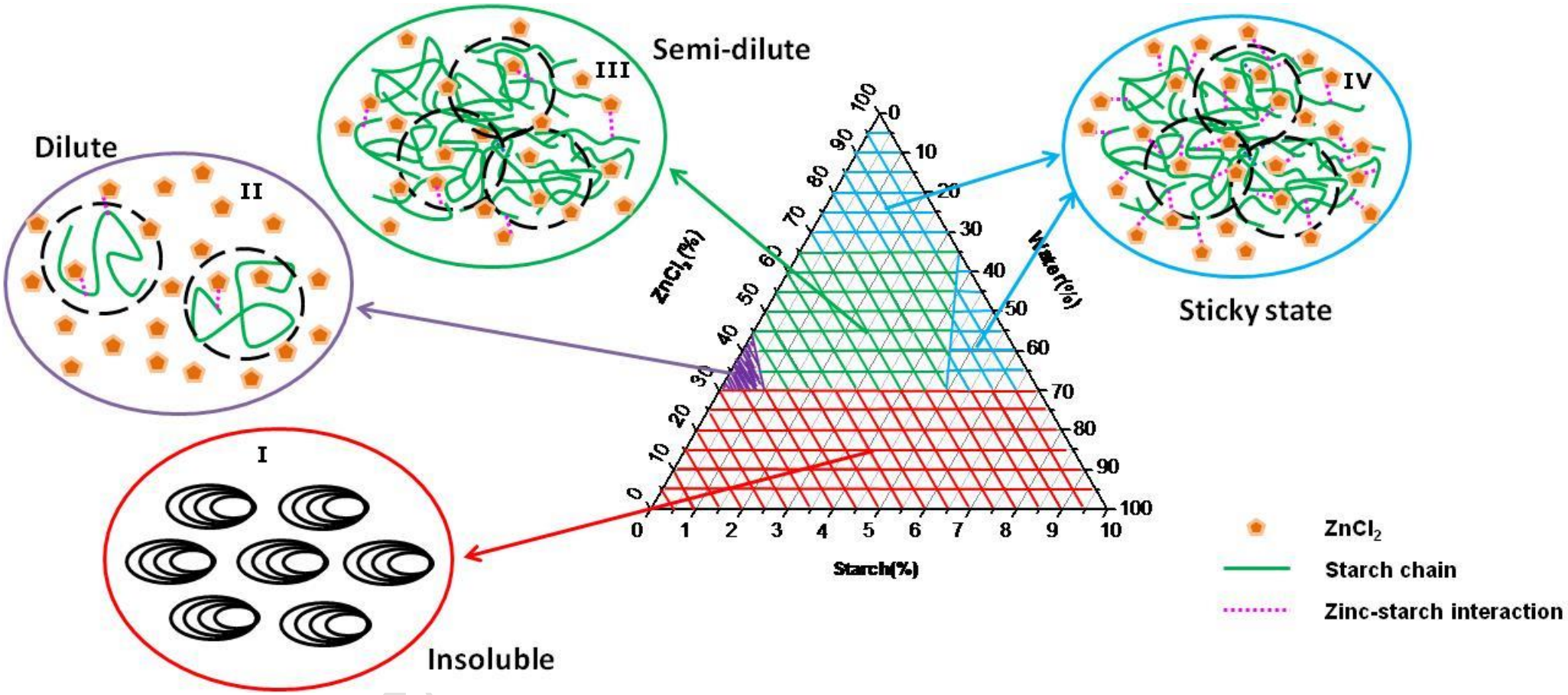

Fig. 4. Phase diagram and schematic representation for cassava starch in $ZnCl_2$ aqueous solutions under different conditions. Phase I represents the "insoluble region"; Phase II represents the "dilute region"; Phase III represents the "semi-dilute region"; and Phase IV represents the "sticky region".

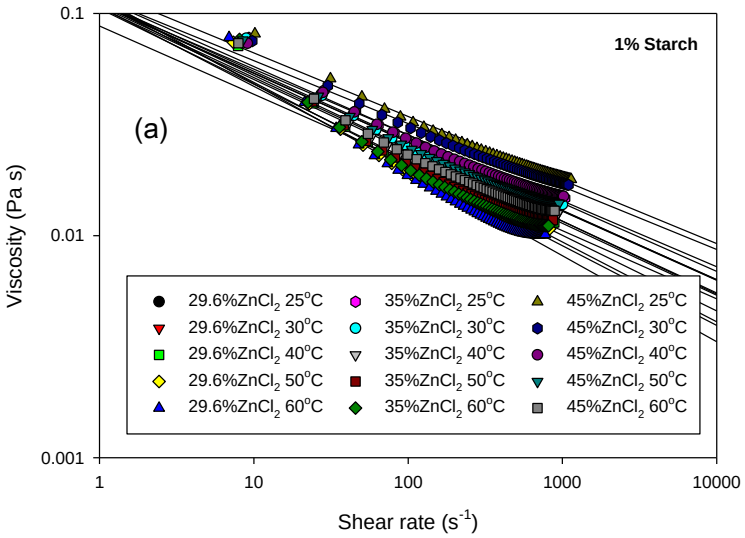

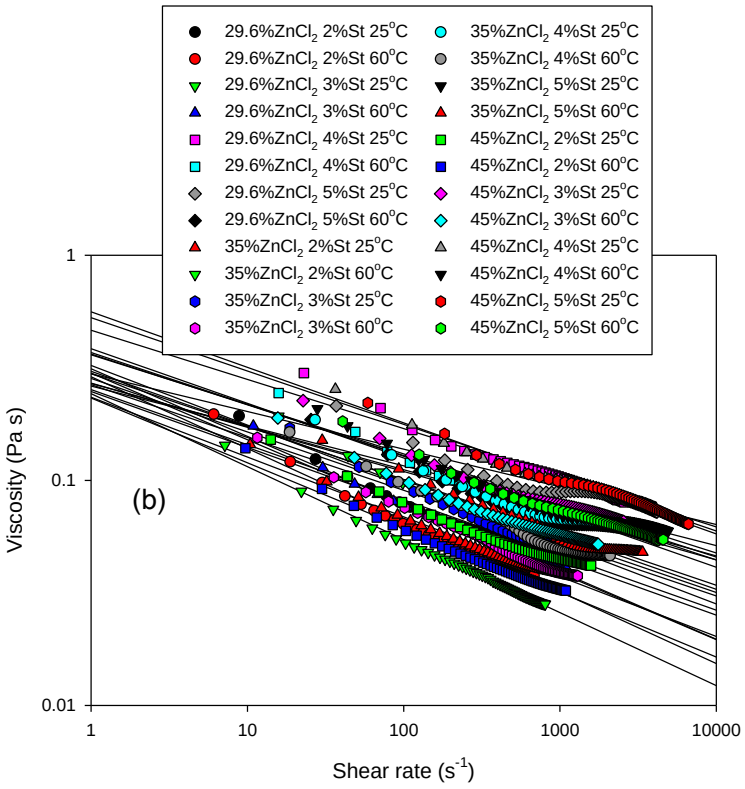

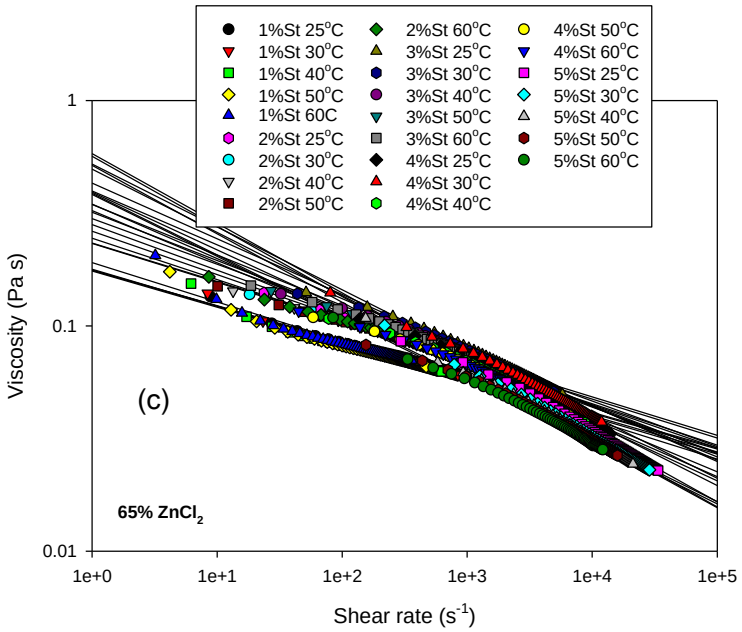

(c)

Fig. 5. Re-built master curves for cassava starch in $ZnCl_2$ solvents in three phase regions. (a) dilute region; (b) semi-dilute region; and (c) sticky region.